Accurate identification of motor unit discharge patterns from high-density surface EMG and validation with a novel signal-based performance metric

2014 J. Neural Eng. 11 016008

(http://iopscience.iop.org/1741-2552/11/1/016008)

IOP Publishing Journal of Neural Engineering
J. Neural Eng. **11** (2014) 016008 (11pp) doi:10.1088/1741-2560/11/1/016008

Accurate identification of motor unit discharge patterns from high-density surface EMG and validation with a novel signal-based performance metric

A Holobar[1,4], **M A Minetto**[2] **and D Farina**[3]

[1] Faculty of Electrical Engineering and Computer Science, University of Maribor, Maribor, Slovenia
[2] Division of Endocrinology, Diabetology and Metabolism, Department of Medical Sciences, University of Turin, Turin, Italy
[3] Department of Neurorehabilitation Engineering, Bernstein Focus Neurotechnology Göttingen, Bernstein Center for Computational Neuroscience, University Medical Center Göttingen, Georg-August University, Göttingen, Germany

E-mail: ales.holobar@uni-mb.si

Received 8 August 2013, revised 8 December 2013
Accepted for publication 9 December 2013
Published 8 January 2014

Abstract

Objective. A signal-based metric for assessment of accuracy of motor unit (MU) identification from high-density surface electromyograms (EMG) is introduced. This metric, so-called pulse-to-noise-ratio (PNR), is computationally efficient, does not require any additional experimental costs and can be applied to every MU that is identified by the previously developed convolution kernel compensation technique. *Approach.* The analytical derivation of the newly introduced metric is provided, along with its extensive experimental validation on both synthetic and experimental surface EMG signals with signal-to-noise ratios ranging from 0 to 20 dB and muscle contraction forces from 5% to 70% of the maximum voluntary contraction. *Main results*. In all the experimental and simulated signals, the newly introduced metric correlated significantly with both sensitivity and false alarm rate in identification of MU discharges. Practically all the MUs with PNR $>$ 30 dB exhibited sensitivity $>$90% and false alarm rates $<$2%. Therefore, a threshold of 30 dB in PNR can be used as a simple method for selecting only reliably decomposed units. *Significance*. The newly introduced metric is considered a robust and reliable indicator of accuracy of MU identification. The study also shows that high-density surface EMG can be reliably decomposed at contraction forces as high as 70% of the maximum.

Keywords: high-density surface EMG, intramuscular EMG, high-force contractions, decomposition, accuracy of motor unit identification

1. Introduction

In vivo investigation of the behaviour of motor units (MUs) provides a unique insight into the neural code underlying movements. Therefore, it has gained interest in several research and clinical areas. This analysis is performed by the decomposition of muscle recordings, typically by means of intramuscular needle or wire electrodes (Mambrito and De Luca 1984, McGill *et al* 2005). However, indwelling electromyography (EMG) is limited to controlled medical environments and usually can be decomposed only for low contraction forces (McGill *et al* 2005, Nawab *et al* 2008).

Muscle activity can also be recorded non-invasively with electrodes placed on the surface of the skin above the muscle of interest (Merletti and Parker 2004, Farina *et al* 2010).

[4] Author to whom any correspondence should be addressed.

This recording modality is less selective than intramuscular EMG but still allows the extraction of complete MU discharge patterns (Holobar and Zazula 2004, 2007, De Luca *et al* 2006, Nawab *et al* 2010, Holobar *et al* 2012b). The non-invasive approach to MU investigation has several advantages over the invasive procedures, as discussed previously (Farina *et al* 2010, Holobar *et al* 2010, Nawab *et al* 2010).

The crucial problem in EMG decomposition is its accuracy. While any algorithm can provide realistic spike trains, the precise quantification of errors in such estimates is elusive (McGill and Marateb 2011). Among the methods for the assessment of accuracy, the inter-operator or inter-algorithm agreement rates (De Luca *et al* 2006, Kleine *et al* 2008) or the agreement between decompositions of different signals containing some sources in common (Holobar *et al* 2010, Nawab *et al* 2010) have been proposed in previous studies. A classic variant of the latter method consists in decomposing one intramuscular and one surface EMG signal concurrently recorded and computing the consistency in discharge time identifications for the MUs extracted from both signals.

All the aforementioned approaches for quantification of the decomposition accuracy suffer from many limitations. Above all, they can only be applied to a set of representative signals to provide a general, and not signal-based, validation of a specific algorithm. Conversely, because of the variability in the interactions between waveforms of MU action potentials, signal artefacts and noise, the accuracy of EMG decomposition needs to be assessed for each individual MU in each signal analysed. Ideally, each decomposed spike train should be reported together with an index of accuracy in its estimation.

Nawab *et al* (2010) proposed a signal-based validation method, named the reconstruct-and-test procedure. However, this method measures the consistency rather than the accuracy of the decomposition (Farina and Enoka 2011, De Luca and Nawab 2011). Another signal-based approach has been proposed for the decomposition of indwelling EMG signals by McGill *et al* (McGill and Marateb 2011) and utilizes statistical decision theory and a Bayesian framework to integrate the information on MU action potential waveform and MU discharge patterns. This procedure is computationally expensive and currently not applicable to more than eight identified MUs.

In this study, we focus on the decomposition of high-density surface EMG by the previously introduced convolution kernel compensation (CKC) method (Holobar and Zazula 2004, 2007). This method has been previously validated for representative simulated and experimental signals at low contraction forces (Holobar *et al* 2010). In this study, we prove that the CKC decomposition can provide precise decomposition also at high forces of isometric contractions, so that we extend the potential applications of this method to practically any contraction level. This proof is obtained by comparison with intramuscular EMG decomposition as well as by a novel metric for signal-based accuracy estimation, which is analytically derived in this manuscript and which constitutes a second contribution of the study. The proposed metric of accuracy, built on linear estimation theory, provides a computationally inexpensive and reliable indicator of the mean square error (MSE) between the true discharge pattern of each identified MU and its CKC-based estimation. In the present study, it will be shown by simulations and experimental signal analysis that this metric correlates significantly with both the sensitivity of the identified MU discharges and their false alarm rates.

2. Methods

2.1. CKC-based identification of MU discharge pattern and corresponding MSE

Under the assumption of isometric muscle contraction and short-term MU action potential stationarity, the A/D-converted multichannel surface EMG can be modelled by (Holobar and Zazula 2004):

$$\mathbf{y}(n) = \mathbf{H}\bar{\mathbf{t}}(n) + \omega(n), \tag{1}$$

where $\mathbf{y}(n) = [y_1(n), \ldots, y_M(n)]^T$ is a vector of M EMG channels, $\omega(n) = [\omega_1(n), \ldots, \omega_M(n)]^T$ is a zero-mean, independent and identically distributed (i.i.d.) noise vector with variance $\sigma^2\mathbf{I}$ and $\bar{\mathbf{t}}(n) = [t_1(n), t_1(n-1), \ldots, t_1(n-L+1), \ldots, t_N(n), \ldots, t_N(n-L+1)]^T$ stands for a vectorized block of L samples from all the MU discharge patterns. The discharge pattern of the jth MU is defined as

$$t_j(n) = \sum_{k=-\infty}^{\infty} \delta[n - \tau_j(k)], \quad j = 1, \ldots, N. \tag{2}$$

where $\delta(\cdot)$ is the unit-sample pulse and the kth action potential of the jth MU appears at time $\tau_j(k)$.

The $M \times NL$ mixing matrix $\mathbf{H}$ comprises all the L-sample long MU action potentials as detected by the surface electrodes:

$$\mathbf{H} = [\mathbf{H}_1 \ \mathbf{H}_2 \ \ldots \ \mathbf{H}_N] \tag{3}$$

with

$$\mathbf{H}_j = \begin{bmatrix} h_{1j}(0) & \cdots & h_{1j}(L-1) \\ h_{2j}(0) & \cdots & h_{2j}(L-1) \\ \vdots & & \vdots \\ h_{Mj}(0) & \cdots & h_{Mj}(L-1) \end{bmatrix} \tag{4}$$

and $h_{ij}(n)$ standing for the nth sample of the jth MU action potential as detected by the ith uptake electrode.

The CKC estimate of the jth MU discharge pattern is given by (Holobar and Zazula 2007)

$$\hat{t}_j(n) = \mathbf{c}_{t_j\mathbf{y}}^T \mathbf{C}_{\mathbf{yy}}^{-1} \mathbf{y}(n), \tag{5}$$

where $\mathbf{C}_{\mathbf{yy}} = E(\mathbf{y}(n)\mathbf{y}^T(n))$ is the correlation matrix of the vector of EMG measurements, $\mathbf{c}_{t_j\mathbf{y}} = E(t_j(n)\mathbf{y}^T(n))$ is the cross-correlation vector between the jth MU discharge pattern and vector $\mathbf{y}(n)$ and $E(.)$ stands for mathematical expectation. In order to increase the decomposition performance (Holobar and Zazula 2007), the vector $\mathbf{y}(n)$ may be substituted by a vectorized block of K samples from all EMG measurements $\bar{\mathbf{y}}(n) = [y_1(n), y_1(n-1), \ldots, y_1(n-K+1), \ldots, y_M(n), \ldots, y_M(n-K+1)]^T$.This modifies the mixing matrix $\mathbf{H}$ in (4), but does not change the theoretical derivations presented herein.

As demonstrated in appendix A, the MSE between the true and CKC-estimated discharge pattern of the jth MU can be asymptotically approximated by

$$E((t_j - \hat{t}_j)^2) = \mathbf{B}_{jj} \tag{6}$$

where $\mathbf{B} = \sigma^2(\sigma^2\mathbf{C}_\mathbf{t}^{-1} + \mathbf{H}^T\mathbf{H})^{-1}$.

Neither $E((t_j - \hat{t}_j)^2)$ nor $\mathbf{B}_{jj}$ can be estimated directly. However, as demonstrated in appendix B, an efficient indication of MSE can be attained by calculating the so-called pulse-to-noise-ratio (PNR):

$$\begin{aligned}\mathrm{PNR}(j) = \mathrm{PNR}(\hat{t}_j(n)) &= 10 \cdot \log\left(\frac{E\left(\hat{t}_j^2(n)|_{\hat{t}_j(n)\geqslant r}\right)}{E\left(\hat{t}_j^2(n)|_{\hat{t}_j(n)<r}\right)}\right) \\ &\approx 10 \cdot \log\left(1 + \frac{c_{t_jt_j} - \mathbf{B}_{jj}}{c_{t_jt_j}\mathbf{B}_{jj}}\right),\end{aligned} \tag{7}$$

where $E(x|_{\hat{t}_j(n)\geqslant r})$ and $E(x|_{\hat{t}_j(n)<r})$ denote the mean across all time moments in which the jth MU is estimated to have or not to have discharged, respectively (appendix B). Note that $\lim_{\sigma\to 0}(\mathbf{B}) = \mathbf{0}$ and $\lim_{\sigma\to\infty}(\mathbf{B}) = \mathbf{C_{tt}}$. Thus, $\lim_{\sigma\to 0}(\mathrm{PNR}(\hat{t}_j(n))) = \infty$ and $\lim_{\sigma\to\infty}(\mathrm{PNR}(\hat{t}_j(n))) = 0$.

2.2. Simulated signals

The efficiency of the proposed PNR and its correlation with sensitivity and false alarm rates in identification of individual MUs were first systematically tested on synthetic high-density surface EMG signals. A muscle with elliptical cross-section of 30 mm (transversal) × 15 mm (depth) and the average fibre length of 130 mm was simulated by a multilayer cylindrical volume conductor model (Farina *et al* 2004), comprising four layers (bone, muscle, fat, skin). Limb and bone radius were set equal to 50 and 25 mm, respectively. Thickness of skin and subcutaneous layer were 1 and 4 mm, respectively. The MU properties across the active MU pool were distributed according to the size principle (Henneman 1957), and included innervation number of 24–2408 fibres per MU, recruitment thresholds with range between 0% and 80% of maximal excitation level (Kukulka and Clamann 1981) and normally distributed conduction velocity values of MU action potentials with mean of 4.0 ± 0.3 m s^{-1}. The muscle comprised a total of 500 MUs (Keenan *et al* 2005) randomly distributed within its cross-section with a density of 20 fibres mm^{-2} (Armstrong *et al* 1988). The simulation of the intracellular action potential was based on the analytical description of Rosenfalck (1969).

The recruitment of a population of MUs was based on the model proposed by Fuglevand *et al* (1993). Three levels of constant excitation to the muscle were simulated: 30%, 50% and 70% of maximum excitation level. The distribution of recruitment thresholds for the motor neurons was modelled with an exponential function with many low-threshold neurons and progressively fewer high-threshold neurons, as described by Fuglevand *et al* (1993). The number of MUs active at 30% (50%, 70%) of maximum excitation level was 388 (446, 484). Each MU discharged at 8 pulses per second (pps) when initially recruited and linearly increased its discharge rate with excitation (0.3 pps/%). The peak discharge rate was 35 pps for all simulated MUs. Discharge rate variability was modelled as a Gaussian random process with coefficient of variation of the inter-spike interval (ISI) equal to 20% (Fuglevand *et al* 1993).

The MU action potentials have been simulated as detected by a bidimensional detection system of 90 electrodes (9 columns, 10 rows) with radius of 1 mm and inter-electrode distance of 5 mm. A bipolar recording was simulated for each longitudinal pair of adjacent electrodes, thus leading to 81 simulated detection points. The centre of the grid was over the centre of the muscle body in the longitudinal and transverse directions. The surface-recorded MU potential was the sum of the action potentials of the muscle fibres belonging to the MU. EMG signals of length of 10 s were computed at 4096 samples s^{-1} and downsampled to 2048 samples s^{-1}. Coloured zero-mean Gaussian noise with signal-to-noise ratio (SNR) 0–20 dB (5 dB increments) and bandwidth 20–500 Hz was added to the simulated recordings.

2.3. Experimental signals

For experimental signals the true spike trains are not known. A conservative estimation of accuracy was thus obtained by comparing intramuscular and surface EMG decompositions. This estimation of accuracy was then compared with the proposed signal-based index.

Nine healthy men (range, age: 24–36 years; stature 1.67–1.80 m; body mass 61–90 kg) participated in the experiment. The subjects received a detailed explanation of the study and gave written informed consent prior to participation. The experiments were conducted in accordance with the Declaration of Helsinki and approved by the local ethics committee.

Surface EMG and intramuscular EMG signals were acquired concurrently from the dominant tibialis anterior muscle of the nine subjects and from the dominant biceps brachii muscle of six out of the nine subjects. The 15 s long signals were acquired during isometric constant force contractions at 5%, 10%, 15%, 20% 50%, 60% and 70% of the maximum voluntary contraction (MVC). Each contraction level was repeated twice. Surface EMG signals were acquired in monopolar mode by a bidimensional array of 90 electrodes (LISiN, Politecnico di Torino, Italy, 1 mm in diameter, inter-electrode distance of 5 mm, 11 rows × 9 columns, the central row not used for the surface EMG recordings) with the third row centred over the main innervation zone and the columns approximately aligned with the muscle fibres. Intramuscular EMG signals were recorded in bipolar mode by three pairs of wire electrodes, each pair comprising two 50 μm stainless-steel wires insulated with Formvar (California Fine Wire, Grover Beach, CA) and glued together at the tip with Histoacryl® (B. Braun Aesculap AG, Tuttlingen, Germany). The insulated wires were cut at the tip to expose only their cross-section. Each electrode was inserted with a 25 G needle at the position of central row of surface electrodes and to a depth of a few millimetres below the muscle fascia. The pairs of electrodes were approximately 1 cm apart.

Acquired signals were amplified, band-pass filtered (EMG-USB2 multichannel amplifier, OT Bioelettronica, Torino, Italy, 3 dB bandwidth 10–500 Hz for surface EMG,

0.1–5 kHz for intramuscular EMG) and stored on a computer hard drive at 2048 samples s^{-1} for surface EMG and 10 000 samples s^{-1} for intramuscular EMG.

2.4. Data analysis

Both simulated and experimental signals were decomposed with the CKC method (see Holobar and Zazula (2007) for technical details). For each identified MU, a PNR, as defined in equation (7), was computed. In addition, the decomposition sensitivity as defined in equation (8), and the false alarm rate, as defined in equation (9) were computed:

$$\mathrm{Se}(j) = \frac{\mathrm{TP}_j}{\mathrm{TP}_j + \mathrm{FN}_j}, \tag{8}$$

$$\mathrm{Fa}(j) = \frac{\mathrm{FP}_j}{\mathrm{FP}_j + \mathrm{FN}_j}, \tag{9}$$

where TP_j (true positives) denotes the number of correctly identified discharges for the jth identified MU, FP_j (false positive) is the number of misplaced discharges and FN_j (false negatives) stands for the number of unidentified discharges. Discharge time tolerance was set equal to ± 0.5 ms.

The experimental intramuscular EMG signals were decomposed by the EMGLAB decomposition tool (McGill *et al* 2005). The average discharge rate and the coefficient of variation ($\mathrm{CoV_{ISI}}$) for the ISI, calculated as SD divided by the mean ISI, were computed for each identified MU. In accordance with the analysis in Holobar *et al* (2010), the MUs with irregular discharge pattern ($\mathrm{CoV_{ISI}} > 30\%$) or small MU action potentials were discarded, as they were considered not reliably identified. The pairs of MUs with similar action potential shapes as identified from indwelling EMG have also been classified as unreliable and discarded from further processing.

For MUs that were identified by both decomposition techniques, the sensitivity as defined in equation (8), and false alarm rate, as defined in equation (9), were computed, using the MU discharge patterns identified from intramuscular EMG as a reference. When matching the decomposition results of surface and intramuscular EMG, two MUs were considered commonly identified only if they shared at least 30% of their discharges (Holobar *et al* 2010).

Regression analysis was used to analyse the dependence of PNR, as defined in equation (7), on the decomposition sensitivity Se, as defined in equation (8), and false alarm rate Fa, as defined in equation (9). In the case of PNR versus Se data, a regression line

$$\mathrm{Se}(j) = a_1 + a_2 \log(\mathrm{PNR}(j) - a_3) \tag{10}$$

has been fitted with the nonlinear least-squares fitting method using the trust-region-reflective optimization algorithm. The starting values of parameters a_1, a_2, and a_3 were set to 90, 6 and 25, respectively. In the case of PNR versus Fa, a regression line

$$\mathrm{Fa}(j) = b_1 - b_2 \log(\mathrm{PNR}(j) - b_3) \tag{11}$$

has been fitted with the starting values of the parameters b_1, b_2 and b_3 set to 0.06, 0.06 and 25, respectively. The r^2 metric was used as a measure of goodness of fit.

Table 1. Converged values of line fitting parameters a_i (mean $\pm$ SD), as defined in equation (10), along with the r^2 measure of goodness of fit. Results are averaged over five different realizations of noise with SNR ranging from 0 to 20 dB.

Excitation level (%)	a_1	a_2	a_3	r^2
30	90.8 ± 3.8	8.8 ± 3.9	24.0 ± 0.8	0.71 ± 0.06
50	87.0 ± 5.2	12.6 ± 5.6	22.4 ± 0.6	0.69 ± 0.19
70	89.0 ± 4.9	10.5 ± 4.8	22.7 ± 1.2	0.78 ± 0.08

Table 2. Converged values of line fitting parameters b_i (mean $\pm$ SD), as defined in equation (11), along with the r^2 measure of goodness of fit. Results are averaged over five different realizations of noise with SNR ranging from 0 to 20 dB.

Excitation level (%)	b_1	b_2	b_3	r^2
30	0.06 ± 0.02	0.06 ± 0.02	24.3 ± 0.6	0.78 ± 0.05
50	0.11 ± 0.05	0.10 ± 0.05	22.7 ± 1.4	0.82 ± 0.09
70	0.11 ± 0.05	0.11 ± 0.05	22.8 ± 1.2	0.73 ± 0.10

3. Results

3.1. Synthetic signals

The cumulative number of identified MUs as a function of sensitivity in the estimation of their discharge patterns and false alarm rates is depicted in figure 1. The results are averaged over ten Monte Carlo simulations of a muscle. In each simulation run, the locations of the MUs within the muscle tissue were randomly selected.

At SNR of 20 dB and excitation levels of 30%, 50% and 70% of maximum excitation discharges of 18 ± 2, 16 ± 1 and 16 ± 2 MUs were identified with sensitivity Se $\geqslant$ 95% from synthetic surface EMG. With 10 dB SNR, these figures decreased to 15 ± 2, 16 ± 2 and 16 ± 2 MUs. The false alarm rate Fa over these MUs was 0.02 ± 0.01% (average over all excitation levels), with a range 0–0.09%.

The dependences of decomposition sensitivity Se and of false alarm rate Fa on PNR are depicted in figures 2 and 3, respectively. The final (converged) values of regression parameters a_i, as defined in equation (10), and parameters b_i, as defined in equation (11), are listed in tables 1 and 2, respectively, along with the average r^2 values.

3.2. Experimental signals

An example of surface EMG recorded from the representative tibialis anterior muscle during its contraction at 70% MVC is depicted in figure 4, along with the sum of MUAP trains identified from the surface EMG by the CKC decomposition technique. A high level of interference between different MU action potentials in the detected surface EMG prevents the use of classic indirect measures of decomposition accuracy, such as matching of an action potential templates to the detected signal waveform, that are commonly used in the case of indwelling EMG.

Figure 5 shows a representative example of discharge patterns and smoothed discharge rates for 24 MUs identified

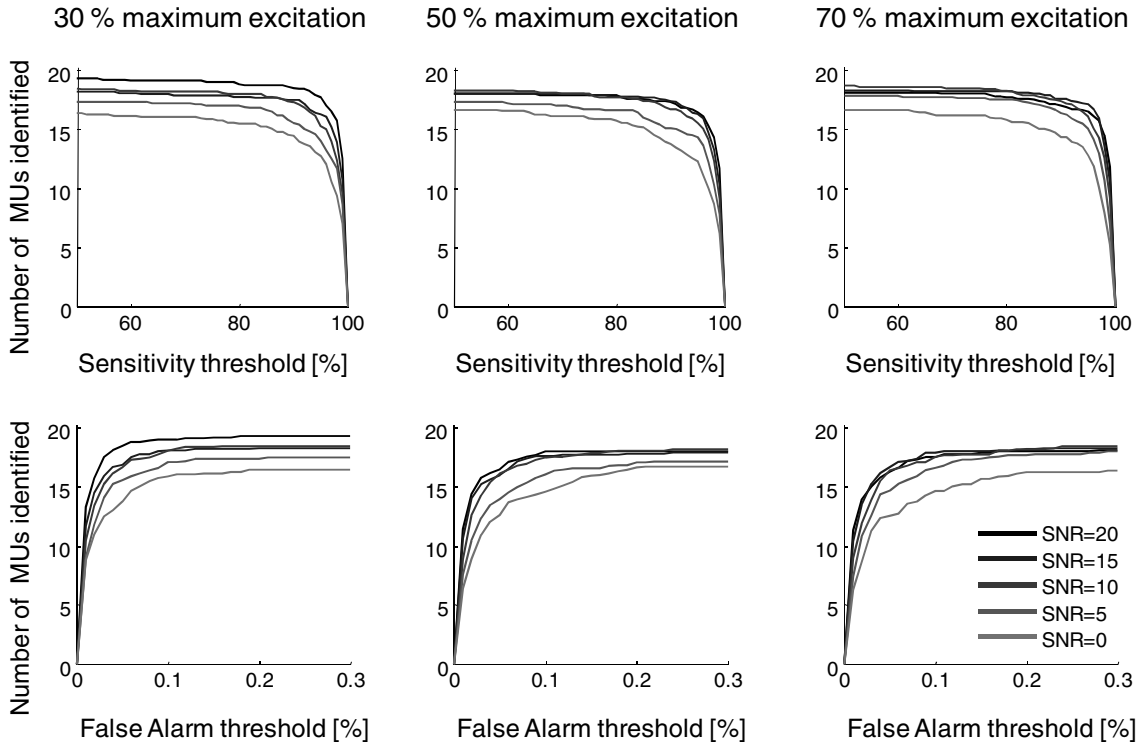

Figure 1. Cumulative number of identified MUs as a function of sensitivity and false alarm rate in the estimation of their discharge patterns, as defined in equations (8) and (9), respectively. The results are averaged over ten Monte Carlo simulations of surface EMG with SNR ranging from 0 to 20 dB and excitation levels of 30%, 50% and 70% of maximum excitation.

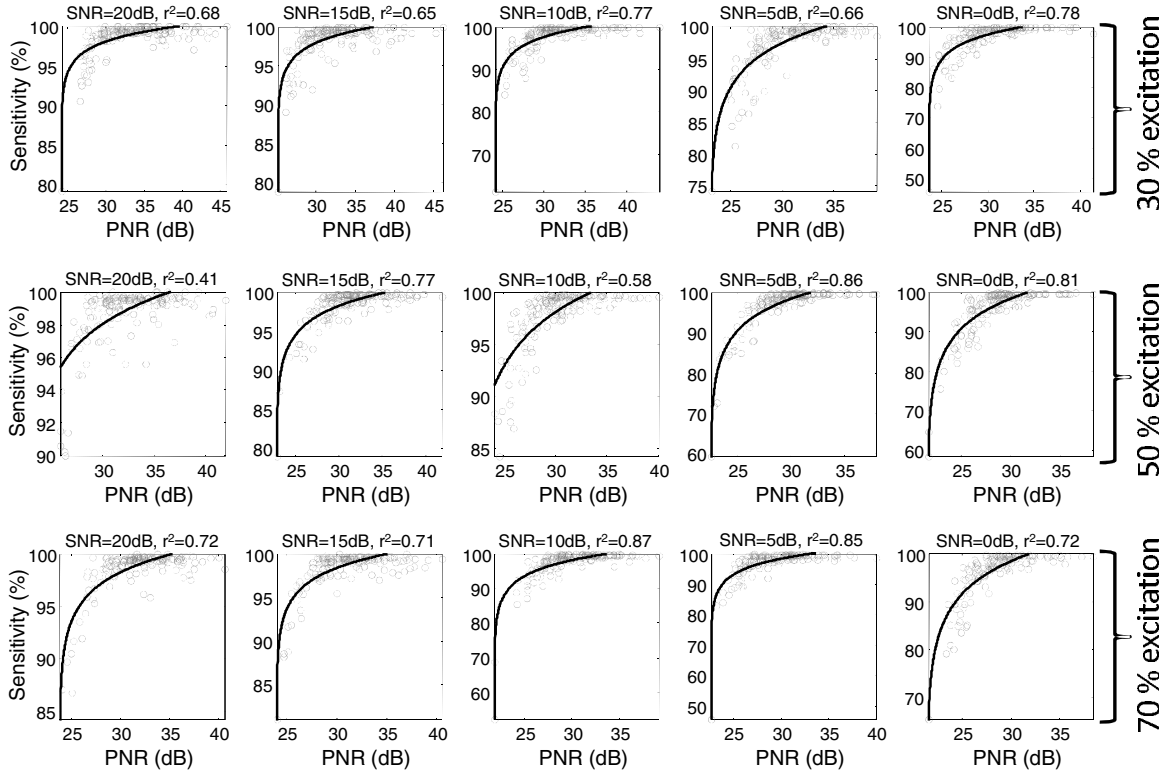

Figure 2. Sensitivity in the CKC-based estimation of MU discharge patterns, as defined in equation (8), as a function of PNR for different excitation levels and different SNRs. The results are accumulated over ten Monte Carlo simulations of surface EMG. Note the different scales on vertical and horizontal axes.

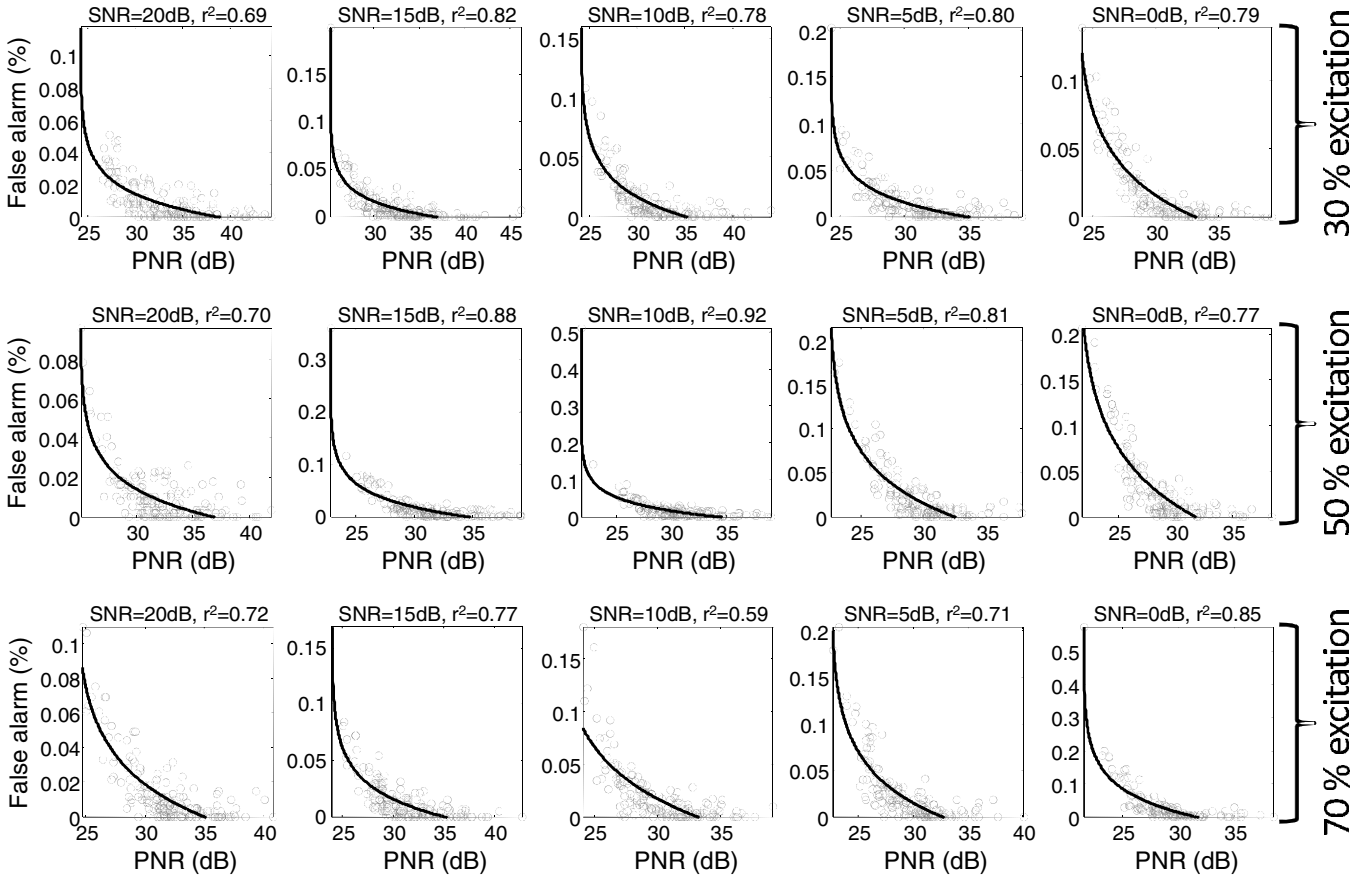

Figure 3. False alarm rate in the CKC-based estimation of MU discharge patterns, as defined in equation (9), as a function of PNR for different excitation levels and different SNRs. The results are accumulated over ten Monte Carlo simulations of surface EMG. Note the different scales on vertical and horizontal axes.

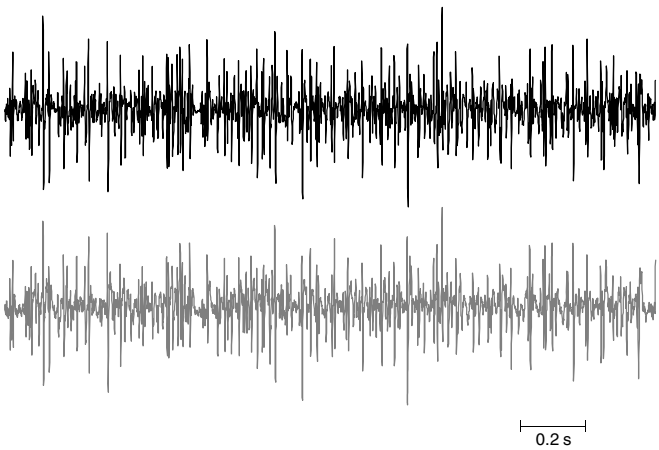

Figure 4. Surface EMG from tibialis anterior muscle during its 70% MVC contraction (black) and the sum of MU action potential trains identified from surface EMG by CKC decomposition technique (grey).

from the surface EMG of the tibialis anterior muscle during its isometric contraction at 70% MVC.

In total, 1314 and 748 MUs were identified from the surface EMG of the tibialis anterior and biceps brachii muscle, respectively. Average discharge rate was a function of the contraction intensity. In fact, in the tibialis anterior it ranged between 11.5 ± 2.1 pps at 5% MVC and 23.2 ± 3.0 pps at 70% MVC. Similarly, in the biceps brachii the MU discharge rate ranged between 12.4 ± 2.3 pps at 5% MVC and 20.3 ± 2.9 pps at 70% MVC.

Due to the strict selection criteria applied to the results of the intramuscular decomposition, only 92 (tibialis anterior) and 60 (biceps brachii) of these MUs were also identified by intramuscular EMG. Average discharge rate of the tibialis anterior MUs ranged between 12.4 ± 2.8 pps at 5% MVC and 21.5 ± 3.1 pps at 70% MVC and that of the biceps brachii MUs ranged between 12.6 ± 3.0 pps at 5% MVC and 20.1 ± 3.9 pps at 70% MVC.

The dependence of PNR on decomposition sensitivity Se and false alarm rate Fa, as defined in equations (8) and (9), respectively, is depicted in figure 6. The distribution of PNR in MUs identified from the surface EMG (for six out of seven contraction levels) is depicted in figures 7 and 8.

4. Discussion

Reliable identification of MU behaviour is a long-standing problem that has been addressed in several previous studies (Nawab *et al* 2008, 2010, Holobar *et al* 2010, McGill and Marateb 2011). The approaches proposed up to now suffer from at least one of the following constraints: computational complexity, invasiveness, lack of the accuracy assessment for every identified MU. These constraints limit the everyday

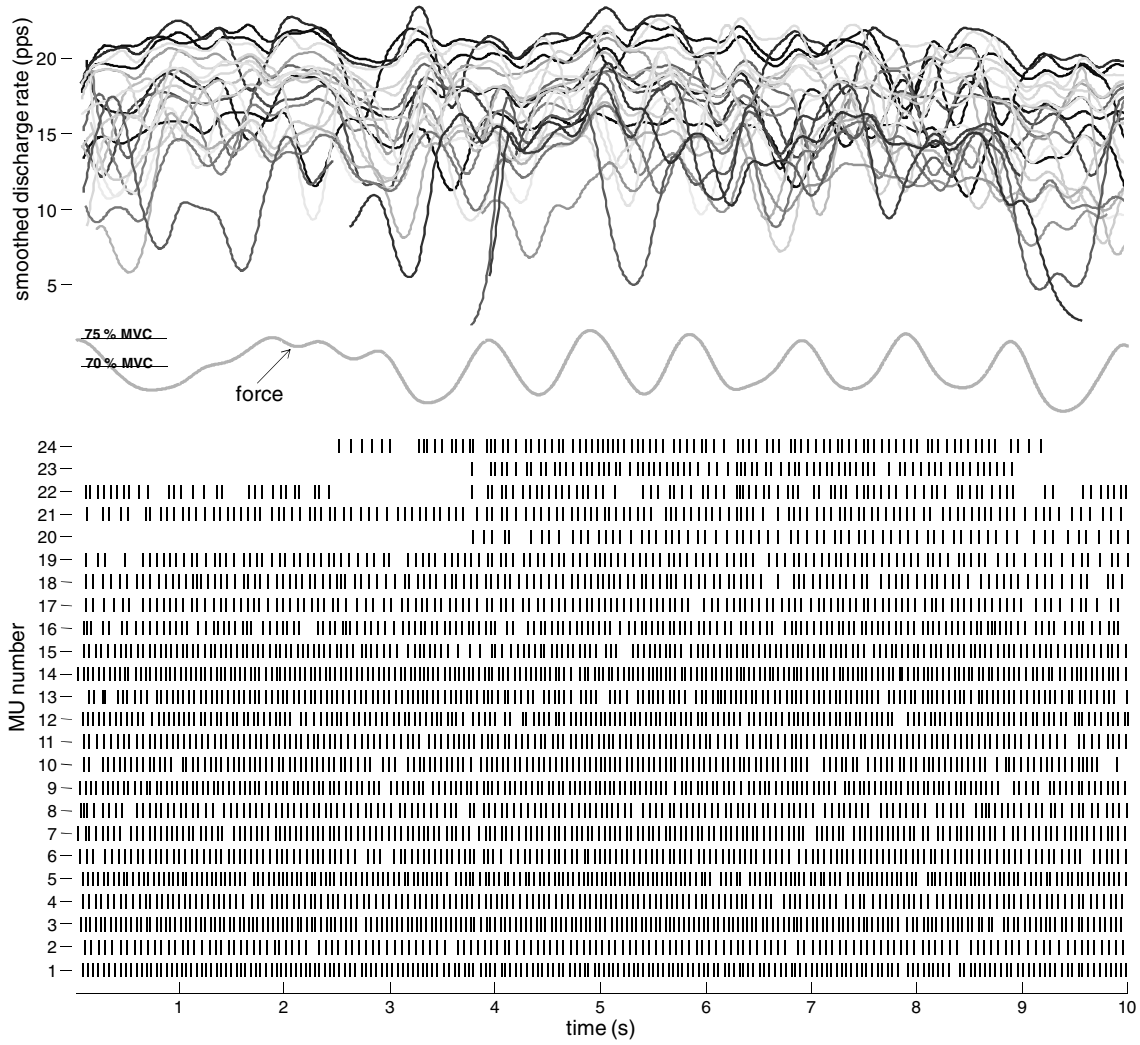

Figure 5. Smoothed discharge rates (upper panel) and discharge patterns (lower panel) of 24 MUs identified by CKC decomposition technique from surface EMG of the tibialis anterior muscle during an isometric constant force contraction at 70% of MVC. Each vertical line in the lower panel indicates a MU discharge at a given time instant. Each thin line in the upper panel corresponds to one MU. Smoothed discharge rates were calculated by low-pass filtering the instantaneous discharge rate, with the cut-off frequency set equal to 2 Hz.

use of surface EMG decomposition in clinical practice and neurophysiologic investigations and also the standardization of examinations on large cohorts of patients.

In this study, a computationally effective measure of surface EMG decomposition accuracy has been introduced. This measure depends on the signal properties and effectively combines all the available information about the MU action potential shapes, without the need for their direct estimation. Moreover, it does not rely on the MU discharge properties and can potentially be used for assessment of decomposition accuracy also in the case of pathologies, such as Parkinsonian and essential tremor (Holobar *et al* 2012a), where the regularity of a MU discharge pattern cannot be guaranteed.

As demonstrated by the results on both synthetic and experimental surface EMG signals, the introduced PNR measure correlates significantly with both the sensitivity and false alarm rate in the identification of MU discharges. As experimentally verified in this study, the majority of MUs with PNR above 30 dB exhibited sensitivity greater than 90% and false alarm rate lower than 1%. This relation was largely independent of the tested signal-to-noise levels (from 0 to 20 dB) and contraction levels (from 5% to 70% MVC).

In order to better elucidate the relationship between the proposed PNR measure and the sensitivity and false alarm rate in identification of MU discharges, the logarithmic curves defined in equations (10) and (11) have been fitted to both decompositions of synthetic and experimental signals. In the case of synthetic signals, the r^2 measure of goodness of fit ranged between 0.41 and 0.92 (figures 2 and 3) with an average value of 0.75 ± 0.10. The worst fit ($r^2 = 0.41$) was in the case of 20 dB SNR and 50% excitation level, where all the MUs were identified with sensitivity above 90% (figure 2). In the case of lower SNRs and, thus, larger range of both PNRs and decomposition sensitivities, the logarithmic fitting produced relatively good matches. Moreover, the values of regression parameters a and b, as defined in equations (10) and (11), did not vary significantly across the different levels of SNR and muscle excitation (tables 1 and 2), allowing for a relatively robust abstraction of a general relation between the introduced

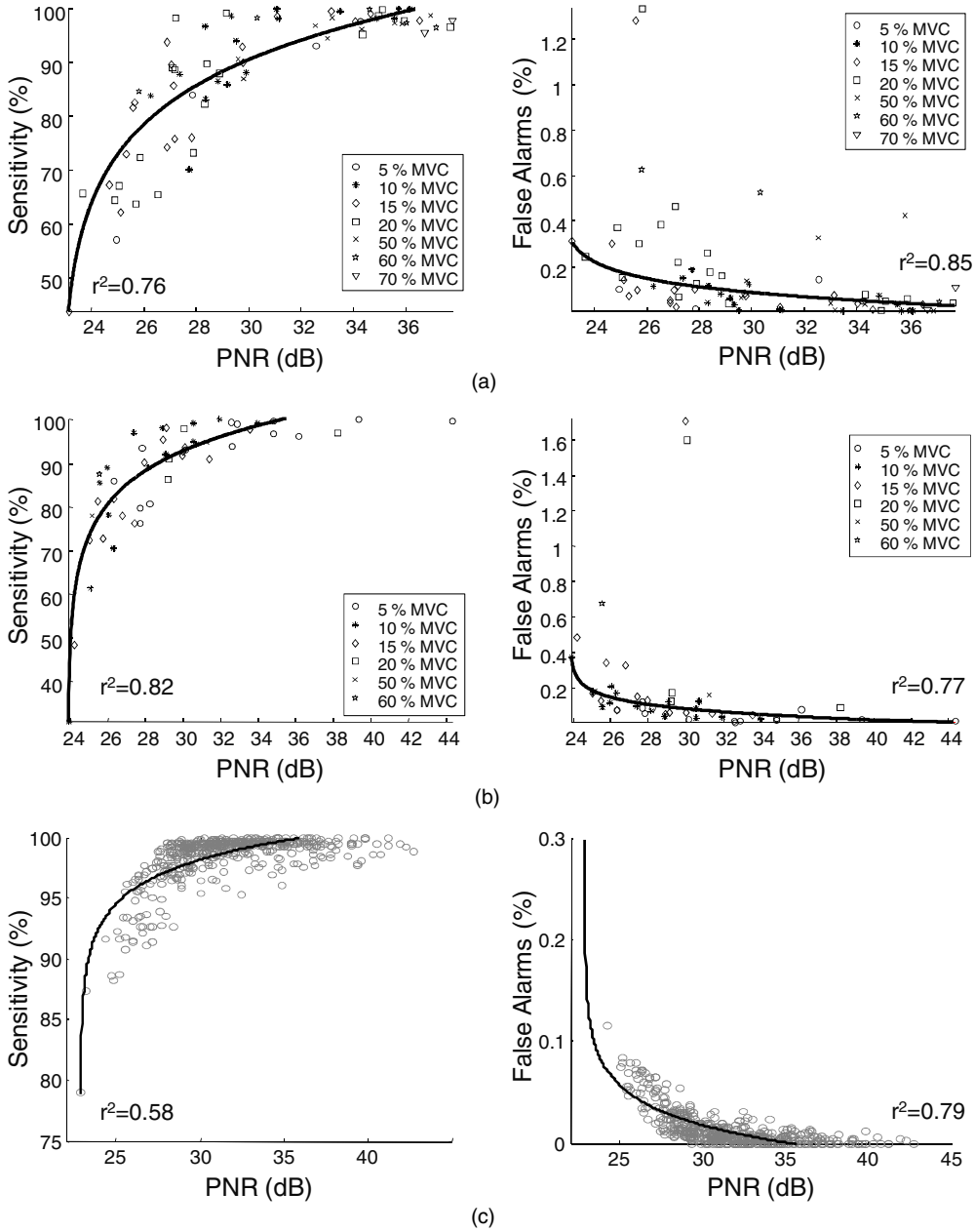

Figure 6. Sensitivity and false alarm rate in the CKC-based estimation of MU discharge patterns, as defined in equations (8) and (9), respectively, as a function of PNR for different contraction levels of tibialis anterior (panels (a)) and biceps brachii muscle (panels (b)). The results are accumulated over all contractions in all the examined subjects. For comparison, the results of simulations, accumulated over all simulated excitation levels at SNR of 15 dB are depicted in panels (c).

PNR measure and decomposition sensitivities and false alarm rates of every identified MU.

Similar results have been demonstrated also with experimental surface EMG. In this case, with no ground truth about the MU discharge patterns, the MUs identified by the EMGLAB decomposition tool (McGill *et al* 2005) from simultaneously acquired indwelling EMG have been selected as reference values. The selection of reliably estimated MUs was performed by an experienced expert, independently of the surface EMG decomposition results. The selection criteria were very strict, discarding any MU with large discharge rate variability ($CoV_{ISI} > 30\%$), small action potential and/or action potential shapes similar to action potentials of other concurrently active MUs. Although conservative and resulting in only 92 (tibialis anterior) and 60 (biceps brachii) identified MUs, such a strict selection was necessary in order to minimize the impact of errors in the decomposition of indwelling EMG on assessment of PNR measure in the experimental conditions (Holobar *et al* 2010).

Due to the low number of MUs that were simultaneously identified from both surface and indwelling EMG, the testing of the PNR-sensitivity and PNR-false alarm rate relationships has been performed on merged decomposition results from all tested contraction levels and all subjects per investigated muscle (figure 6). As in the case of synthetic signals, the logarithmic curve fitting defined in equations (10) and (11)

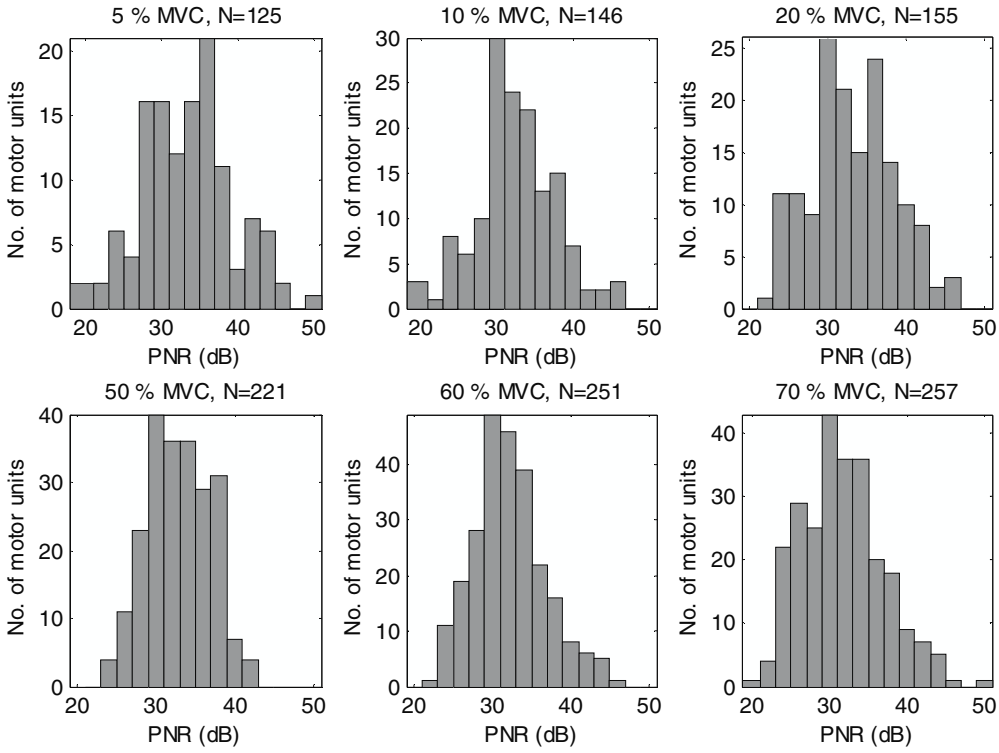

Figure 7. Distribution of PNR of all the MUs identified from the surface EMG of tibialis anterior muscle at different contraction levels. The results are accumulated over nine healthy subjects.

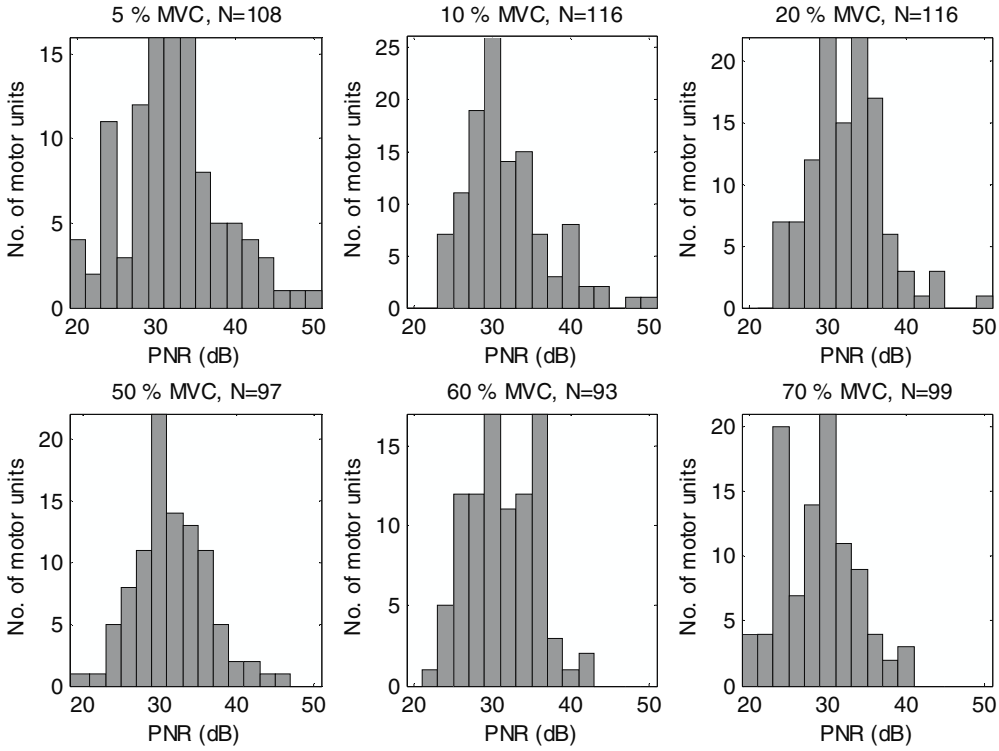

Figure 8. Distribution of PNR of all the MUs identified from the surface EMG of biceps brachii muscle at different contraction levels. The results are accumulated over six healthy subjects.

has been applied. In the case of PNR-sensitivity matching, the r^2 measure of goodness of fit yielded 0.74 (tibialis anterior) and 0.79 (biceps brachii). For PNR-false alarm rate matching, the r^2 yielded 0.87 (tibialis anterior) and 0.81 (biceps brachii). These results are comparable to the ones on synthetic EMG signals, also when decomposition results are accumulated across different contraction levels (figure 6). Also similarly to the case of synthetic signals, experimentally identified MUs with PNR $>$ 30 dB exhibited sensitivity $>$ 90% and false alarm rate below 2%.

In all the contractions together, 879 out of 1314 (tibialis anterior) and 449 out of 748 (biceps brachii) MUs identified from surface EMG exhibited PNR > 30 dB (figures 7 and 8). As demonstrated by the extensive results of this study, it is reasonable to assume that all these MUs were identified with sensitivity above 90%. Moreover, 1126 out of 1314 (tibialis anterior) and 613 out of 748 (biceps brachii) MUs were identified with PNR > 28 dB, which corresponds to a sensitivity above 85% (figures 6–8). The distribution of PNR was not significantly influenced by muscle contraction level (figures 7 and 8). These results are comparable to the results presented in Nawab *et al* (2010) and demonstrate the possibility of accurately decomposing surface EMG signals by CKC in a large force range. On the other hand, the decomposition of indwelling EMG in McGill and Marateb (2011) yielded higher accuracy rates, but on signals with much less interference and higher frequency bandwidth.

Interestingly, the number of identified MUs increased with the contraction level in tibialis anterior muscle (figure 7), but not in the biceps brachii muscle (figure 8). In order to further investigate this phenomenon, the signal-to-interference ratio (SIR), indicating the proportion of the raw surface EMG energy identified by the decomposition, was calculated as in Holobar *et al* (2010). When averaged over contraction levels at 50%, 60% and 70% MVC, the identified MUs accounted for 30.8 ± 12.4% and 29.4 ± 5.4% of the raw EMG energy in tibialis anterior and biceps brachii muscle, respectively. The difference was not statistically significant (Kruskal–Wallis test, $p > 0.05$), thus approximately the same proportion of signal energy was identified in both investigated muscles. In agreement with Holobar *et al* (2010), practically all large MUAPs were identified (figure 4), while MUAPs of small and distant MUs were treated as physiological noise.

The proposed measure of decomposition accuracy is computationally bound to the CKC-based decomposition and high-density surface EMG recordings with several tens of recorded EMG channels (Holobar *et al* 2010). The number of required channels is a function of a number of active MUs in the detection volume and is, thus, application dependent. However, as demonstrated by simulations at 30% excitation (results not shown here), the performance of PNR does not change when the uptake array decreases from 10 × 9 to 6 × 5 electrodes (Holobar *et al* 2013).

It is noteworthy that the CKC method already provided the pulse trains $\hat{t}_j(n)$ and the corresponding threshold r in (7). Thus, when combined with the CKC decomposition method the additional computational costs introduced by PNR are limited to the calculation of the sample means $E(x|_{\hat{t}_j(n)\geqslant r})$ and $E(x|_{\hat{t}_j(n)<r})$ in (7). This is significantly less than the costs of a second decomposition run proposed in Nawab *et al* (2010), for example, or the signal-based approach proposed by McGill and Marateb (2011). Although possible, the extension of PNR metric to other decomposition techniques is less practical and results in additional computational costs as the basic decomposition steps of CKC have to be performed. Thus, the proposed measure cannot easily be generalized to other EMG decomposition techniques.

In summary, a computationally efficient PNR measure for reliable and robust assessment of accuracy in identification of each MU by CKC-based decomposition has been introduced. The measure exhibits strong correlation with both sensitivity and false alarm rates in the identification of MU discharges. In this study, all MUs with PNR > 30 dB exhibited sensitivity > 90% and false alarm rates <2%, regardless of the signal modality (synthetic or experimental), muscle contraction level (from 5% to 70% MVC) or simulated noise level (from 0 to 20 dB).

Acknowledgments

The authors are grateful to Dr Alberto Botter (Politecnico di Torino, Italy) for valuable assistance in the experimental measures. This study was supported by the Commission of the European Union, within Framework 7, under grant agreement no. ICT-2011.5.1-287739 'NeuroTREMOR: a novel concept for support to diagnosis and remote management of tremor.' (AH), by the bank foundation 'Compagnia di San Paolo' (Project 'Neuromuscular Investigation and Conditioning in Endocrine Myopathies') (MAM) and the European Research Council Advanced Grant DEMOVE (contract no. 267888) (DF).

Appendix A. The mean square error of MU discharge pattern estimation

The MSE of the jth MU discharge pattern estimation (5) can be expressed as

$$\begin{aligned} E((\hat{t}_j - t_j)^2) &= E\left(\hat{t}_j^2 - 2\hat{t}_j t_j + t_j^2\right) \\ &= \mathbf{c}_{\hat{t}_j\mathbf{y}}^T \mathbf{C}_{\mathbf{y}}^{-1} \mathbf{c}_{\hat{t}_j\mathbf{y}} - 2\mathbf{c}_{\hat{t}_j\mathbf{y}}^T \mathbf{C}_{\mathbf{y}}^{-1} \mathbf{c}_{t_j\mathbf{y}} + c_{t_j t_j} \\ &= c_{t_j t_j} + \mathbf{c}_{\hat{t}_j\mathbf{t}}^T (\mathbf{C}_{\mathbf{tt}} + \sigma^2 \mathbf{H}^{-1}\mathbf{H}^{-T})^{-1} (\mathbf{c}_{\hat{t}_j\mathbf{t}} - 2\mathbf{c}_{t_j\mathbf{t}}), \end{aligned} \tag{A.1}$$

where $c_{t_j t_j}$ denotes the (i, j)th element of $\mathbf{C}_{\mathbf{tt}}$. By using the Kailath variant (Bishop 1995, pp 153), we have

$$\begin{aligned} &(\mathbf{C}_{\mathbf{tt}} + \sigma^2 \mathbf{H}^{-1}\mathbf{H}^{-T})^{-1} \\ &= \mathbf{C}_{\mathbf{tt}}^{-1} - \sigma^2 \mathbf{C}_{\mathbf{tt}}^{-1}\mathbf{H}^{-1}\left(\mathbf{I} + \sigma^2 \mathbf{H}^{-T}\mathbf{C}_{\mathbf{tt}}^{-1}\mathbf{H}^{-1}\right)^{-1}\mathbf{H}^{-T}\mathbf{C}_{\mathbf{tt}}^{-1} \\ &= \mathbf{C}_{\mathbf{tt}}^{-1} - \mathbf{C}_{\mathbf{tt}}^{-1}\mathbf{B}\mathbf{C}_{\mathbf{tt}}^{-1}, \end{aligned} \tag{A.2}$$

where $\mathbf{B} = \sigma^2\left(\sigma^2 \mathbf{C}_{\mathbf{tt}}^{-1} + \mathbf{H}^T\mathbf{H}\right)^{-1}$. Thus,

$$E((\hat{t}_j - t_j)^2) = c_{t_j t_j} + \mathbf{c}_{\hat{t}_j\mathbf{t}}^T\left(\mathbf{C}_{\mathbf{tt}}^{-1} - \mathbf{C}_{\mathbf{tt}}^{-1}\mathbf{B}\mathbf{C}_{\mathbf{tt}}^{-1}\right)(\mathbf{c}_{\hat{t}_j\mathbf{t}} - 2\mathbf{c}_{t_j\mathbf{t}}). \tag{A.3}$$

As demonstrated in Holobar *et al* (2012a), CKC converges to $\mathbf{c}_{\hat{t}_j\mathbf{y}} = \mathbf{c}_{t_j\mathbf{y}}$ for $j = 1, \ldots, NL$. Thus, (4) yields

$$E((t_j - \hat{t}_j)^2) = c_{t_j t_j} - \mathbf{c}_{\hat{t}_j\mathbf{t}}^T \mathbf{C}_{\mathbf{t}}^{-1} \mathbf{c}_{t_j\mathbf{t}} + \mathbf{c}_{t_j\mathbf{t}}^T \mathbf{C}_{\mathbf{tt}}^{-1}\mathbf{B}\mathbf{C}_{\mathbf{t}}^{-1}\mathbf{c}_{t_j\mathbf{t}} = \mathbf{B}_{jj}. \tag{A.4}$$

Let $\mathbf{A} = \mathbf{B}^{-1} = \mathbf{C}_{\mathbf{tt}}^{-1} + \sigma^{-2}\mathbf{H}^T\mathbf{H}$ ($\mathbf{A}$ exists only when $\sigma^2 \neq 0$). Then a change $\Delta\mathbf{A}_{\mathrm{rs}}$ of the (r, s)th element of $\mathbf{A}$ results in the following change of the jth diagonal element of $\mathbf{B}$:

$$\Delta\mathbf{B}_{jj} = -\frac{\mathbf{B}_{jr}\mathbf{B}_{sj}\Delta\mathbf{A}_{rs}}{1 + \mathbf{B}_{sr}\Delta\mathbf{A}_{sr}}. \tag{A.5}$$

Note that both $\mathbf{A}$ and $\mathbf{B}$ are symmetric and positive semidefinite, so $\mathbf{B}_{jr}\,\mathbf{B}_{rj} \geqslant 0$ and $\mathbf{B}_{rr} \geqslant 0$. Thus, according to (A.5), MSE decreases when $\Delta\mathbf{A}_{rr} > 0$, i.e. with the increase in the energy of the rth MU's contributions with respect to the contributions of other MUs. Likewise, MSE decreases with the

increase in the cross-correlation between the action potential of the rth MU and action potentials of all other MUs.

Appendix B. Pulse-to-noise ratio

Due to the well-known amplitude ambiguity of blind source separation approaches (Hyvärinen *et al* 2001), the pulses in (5) are of arbitrary amplitude. Thus, the MSE in (A.4) needs to be normalized by the factor $c_{t_jt_j}$. This yields the normalized MSE estimate

$$\mathrm{MSE} = \frac{E((\hat{t}_j - t_j)^2)}{E\left(t_j^2\right)} = \frac{\mathbf{B}_{jj}}{c_{t_jt_j}}. \tag{B.1}$$

In practice, neither $E((\hat{t}_j - t_j)^2)$ nor $E(t_j^2)$ are known. Thus, they have to be replaced by measurable quantities. Analogously to (A.4), we have

$$E\left(\hat{t}_j^2(n)\big|_{t_j(n)=1}\right) = 1 - 2\frac{\mathbf{B}_{jj}}{c_{t_jt_j}} + \mathbf{B}_{jj} + \frac{\mathbf{B}_{jj}^2}{c_{t_jt_j}^2}(1 - c_{t_jt_j}) \tag{B.2}$$

and

$$E\left(\hat{t}_j^2(n)\big|_{t_j(n)=0}\right) = \frac{c_{t_jt_j} - \mathbf{B}_{jj} - c_{t_jt_j}E\left(\hat{t}_j^2(n)\big|_{\hat{t}_j(n)=1}\right)}{1 - c_{t_jt_j}} \tag{B.3}$$

where $E(x|_{t_j(n)=1})$ and $E(x|_{t_j(n)=0})$ denote the mean across all time moments in which the jth MU did and did not discharge, respectively. The left-hand sides in (B.2) and (B.3) can be replaced by $E(x|_{t_j(n)=1}) \approx E(x|_{\hat{t}_j(n)\geqslant r})$ and $E(x|_{t_j(n)=0}) \approx E(x|_{\hat{t}_j(n)<r})$, respectively, where the required threshold r can be estimated for each individual $\hat{t}_j(n)$ by a heuristic penalty function proposed in Holobar *et al* (2012a). As demonstrated by the results of this study, there is a significant difference between the energy of pulses in $\hat{t}_j(n)$ as estimated by (B.2) and the energy of baseline noise as estimated in (B.3). Thus, even a coarse estimate of threshold r suffices for PNR calculation.

Finally, after a short algebraic manipulation of (B.2) and (B.3), the PNR can be defined as in (7).

References

Armstrong J B, Rose P K, Vanner S, Bakker G J and Richmond F J 1988 Compartmentalization of motor units in the cat neck muscle, biventer cervicis *J. Neurophysiol.* **60** 30–45

Bishop C 1995 *Neural Networks for Pattern Recognition* (New York: Oxford University Press)

De Luca C J, Adam A, Wotiz R, Gilmore L D and Nawab S H 2006 Decomposition of surface EMG signals *J. Neurophysiol.* **96** 1646–57

De Luca C J and Nawab S H 2011 Reply to Farina and Enoka: the reconstruct-and-test approach is the most appropriate validation for surface EMG signal decomposition to date *J. Neurophysiol.* **105** 983–4

Farina D and Enoka R M 2011 Surface EMG decomposition requires an appropriate validation *J. Neurophysiol.* **105** 981–2

Farina D, Holobar A, Merletti R and Enoka R M 2010 Decoding the neural drive to muscles from the surface electromyogram *Clin. Neurophysiol.* **121** 1616–23

Farina D, Mesin L, Martina S and Merletti R 2004 A surface EMG generation model with multilayer cylindrical description of the volume conductor *IEEE Trans. Biomed. Eng.* **51** 415–26

Fuglevand A J, Winter D A and Patla A E 1993 Models of recruitment and rate coding organization in motor unit pools *J. Neurophysiol.* **70** 2470–88

Henneman E 1957 Relation between size of neurons and their susceptibility to discharge *Science* **126** 1345–7

Holobar A, Glaser V, Gallego J A, Dideriksen J L and Farina D 2012a Non-invasive characterization of motor unit behaviour in pathological tremor *J. Neural Eng.* **9** 056011

Holobar A, Minetto M A, Botter A and Farina D 2012b Identification of motor unit discharge patterns from high-density surface EMG during high contraction levels *IFMBE Proc.* **37** 1165–8

Holobar A, Minetto M A, Botter A, Negro F and Farina D 2010 Experimental analysis of accuracy in the identification of motor unit spike trains from high-density surface EMG *IEEE Trans. Neural Syst. Rehabil. Eng.* **18** 221–9

Holobar A, Minetto M A and Farina D A 2013 Signal-based approach for assessing the accuracy of high-density surface EMG decomposition *IEEE NER Proc.* pp 585–8

Holobar A and Zazula D 2004 Correlation-based decomposition of surface electromyograms at low contraction forces *Med. Biol. Eng. Comput.* **42** 487–95

Holobar A and Zazula D 2007 Multichannel blind source separation using convolution kernel compensation *IEEE Trans. Signal Process.* **55** 4487–96

Hyvärinen A, Karhunen J and Oja E 2001 *Independent Component Analysis* (New York: Wiley-Interscience)

Keenan K G, Farina D, Maluf K S, Merletti R and Enoka R M 2005 Influence of amplitude cancellation on the simulated surface electromyogram *J. Appl. Physiol.* **98** 120–31

Kleine B U, van Dijk J P, Zwarts M J and Stegeman D F 2008 Inter-operator agreement in decomposition of motor unit firings from high-density surface EMG *J. Electromyogr. Kinesiol.* **18** 652–61

Kukulka C G and Clamann H P 1981 Comparison of the recruitment and discharge properties of motor units in human brachial biceps and adductor pollicis during isometric contractions *Brain Res.* **219** 45–55

Mambrito B and De Luca C J 1984 A technique for the detection, decomposition and analysis of the EMG signal *Electroencephalogr. Clin. Neurophysiol.* **58** 175–88

McGill K C, Lateva Z C and Marateb H R 2005 EMGLAB: an interactive EMG decomposition program *J. Neurosci. Methods* **149** 121–33

McGill K C and Marateb H R 2011 Rigorous a posteriori assessment of accuracy in EMG decomposition *IEEE Trans. Neural Syst. Rehabil. Eng.* **19** 54–63

Merletti R, Aventaggiato M, Botter A, Holobar A, Marateb H and Vieira T M 2010 Advances in surface EMG: recent progress in detection and processing techniques *Crit. Rev. Biomed. Eng.* **38** 305–45

Merletti R and Parker P A 2004 *Electromyography: Physiology, Engineering, and Non-Invasive Applications* (New York: IEEE Press/Wiley)

Nawab S H, Chang S S and De Luca C J 2010 High-yield decomposition of surface EMG signals *Clin. Neurophysiol.* **121** 1602–15

Nawab S H, Wotiz R P and De Luca C J 2008 Decomposition of indwelling EMG signals *J. Appl. Physiol.* **105** 700–10

Rosenfalck P 1969 Intra- and extracellular potential fields of active nerve and muscle fibers *Acta Physiol. Scand. Suppl.* **47** 239–46